International Journal of Electrical and Electronic Engineering & Telecommunications

ISSN 2319 – 2518 www.ijeetc.com
Vol. 5, No. 2, April 2016

Research Paper

A NOVEL CONCEPT OF SIMULTANEOUS VOLTAGE SAG/SWELL AND LOAD REACTIVE POWER COMPENSATIONS UTILIZING SERIES INVERTER OF: IUPQC

Sarvani K[1]* and S K M D Shareef[2]

*Corresponding Author: Sarvani K, ✉ vani.07240@gmail.com

In this paper is proposed a compensation strategy based on a particular CUPS device, the Unified Power Quality Compensator (UPQC). A customized internal control scheme of the UPQC device was developed to regulate the voltage and to mitigate voltage fluctuations at grid side. The internal control strategy is based on the management of active and reactive power in the series and shunt converters of the UPQC, and the exchange of power between converters through UPQC DC-Link. This approach increase the compensation capability of the UPQC with respect to other custom strategies that use reactive power only. Simulations results show the effectiveness of the proposed compensation strategy for the enhancement of Power Quality.

Keywords: UPQC, Active filters, Power line conditioning, Control design

INTRODUCTION

THE usage of power quality conditioners in the distribution system network has increased during the past years due to the steady increase of nonlinear loads connected to the electrical grid. The current drained by nonlinear loads has a high harmonic content, distorting the voltage at the utility grid and consequently affecting the operation of critical loads.

By using a Unified Power Quality Conditioner (UPQC) [1]-[32] it is possible to ensure a regulated voltage for the loads, balanced and with low harmonic distortion and at the same time draining undistorted currents from the utility grid, even if the grid voltage and the load current having harmonic contents. The UPQC consists of two active filters, the Series Active Filter (SAF) and the shunt or Parallel Active Filter (PAF) [1], [2].

The PAF is usually controlled as a non-sinusoidal current source, which is responsible for compensating the harmonic current of the load, while the SAF is controlled as a non-sinusoidal voltage source, which is

[1] M. Tech Student, Narasaraopeta Engineering College, Guntur, Andhra Pradesh 522611, India.

[2] Assistant Professor, Narasaraopeta Engineering College, Guntur, Andhra Pradesh 522611, India.

responsible for compen-sating the grid voltage. Both of them have a control reference with harmonic contents and usually these references might be obtained through complex methods [4], [5], [14], [17], [21], [23], [27].

Some works shows a control technique to the both shunt and SAFs with uses sinusoidal references without the need of harmonic extraction, in order to decrease the complexity of the reference generation for the UPQC [31], [33].

An interesting alternative for power quality conditioners was proposed in [34] and was called Line Voltage Regu-lator/Conditioner (LVRC). This conditioner consists of two single-phase Current Source Inverters (CSI) where the SAF is controlled by a current loop and the PAF is controlled by a voltage loop. In this way, both grid current and load voltage are sinusoidal and therefore their references are also sinusoidal.

Some authors have applied this concept, using Voltage Source Inverters (VSI) in Uninterruptable Power Supplies (UPS) [35], [36] and in UPQC [10], [25], [32]. In [10] this concept is called “dual topology of Unified Power Quality Conditioner” (iUPQC), and the control schemes use the p-q theory requiring determination in real time of the positive sequence components of the voltages and the currents.

The aim of this paper is to propose a simplified control technique for a dual three-phase topology of a Unified Power Quality Conditioner (iUPQC) to be used in the utility grid connection. The proposed control scheme is developed in ABC reference frame and allows the use of classical control theory without the need for coordinate transformers and digital control implementation. The references to both SAF and PAFs are sinusoidal dispensing the harmonic extraction of the grid current and load voltage.

DUAL UNIFIED POWER QUALITY CONDITIONER

The conventional UPQC structure is composed of a SAF and a PAF, as shown in Figure 1. In this configuration the SAF works as a voltage source in order to compensate the grid distortion, unbalances and disturbances like sags, swells and flicker. Therefore, the voltage compensated by the SAF is composed by a fundamental content and by the harmonics. The PAF works as a current source and it is responsible for compensate the unbalances, displacement and harmonics of the load current, ensuring a sinusoidal grid current. The series filter connection to the utility grid is made through a transformer, while the shunt filter is usually connected directly to the load, mainly in low voltage grid applications. The conventional UPQC has the following drawbacks: complex harmonic extraction of the

Figure 1: Conventional Unified Power Quality Conditioner (UPQC)

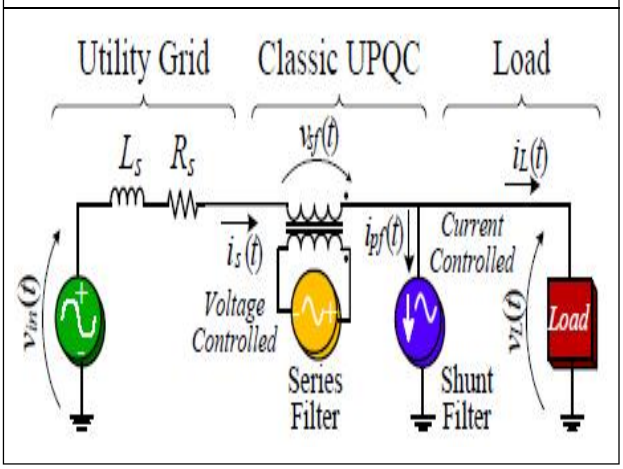

Figure 2: Dual Unified Power Quality Conditioner (iUPQC)

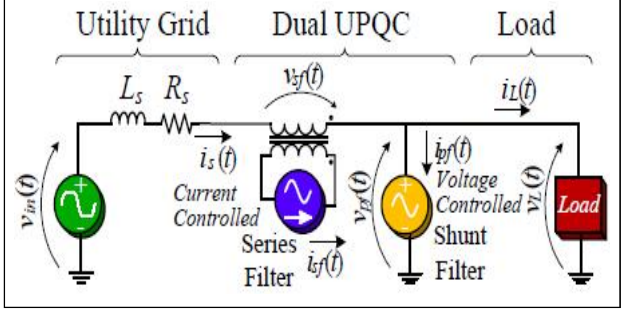

grid voltage and the load involving complex calculations; voltage and current references with harmonic contents requiring a high bandwidth control; the leakage inductance of the series connection transformer affecting the voltage compensation generated by the series filter.

In order to minimize these drawbacks, the iUPQC is in-vestigated in this paper and its scheme is shown in Figure 2. The scheme of the iUPQC is very similar to the conventional UPQC, using an association of the SAF and PAF, diverging only from the way the series and shunt filters are controlled. In the iUPQC the SAF works as a current source, which imposes a sinusoidal input current synchronized with the grid voltage. The PAF works as a voltage source imposing sinusoidal load voltage synchronized with the grid voltage. In this way, the iUPQC control uses sinusoidal references for both active filters. This is a major point to observe related to the classic topology since the only request of sinusoidal reference generation is that it must be synchronized with the grid voltage. The SAF acts as high impedance for the current harmonics, and indirectly compensates the harmonics, unbalances and disturbances of grid voltage since the connection transformer voltages are equals the difference between the grid voltage and load voltage. In the same way, the PAF indirectly compensates the unbalances, displacement and harmonics of the grid current, providing low impedance path for harmonic load current.

POWER CIRCUIT

The power circuit of the proposed iUPQC is made up of two four wire three-phase

Figure 3: Power Circuit of the iUPQC

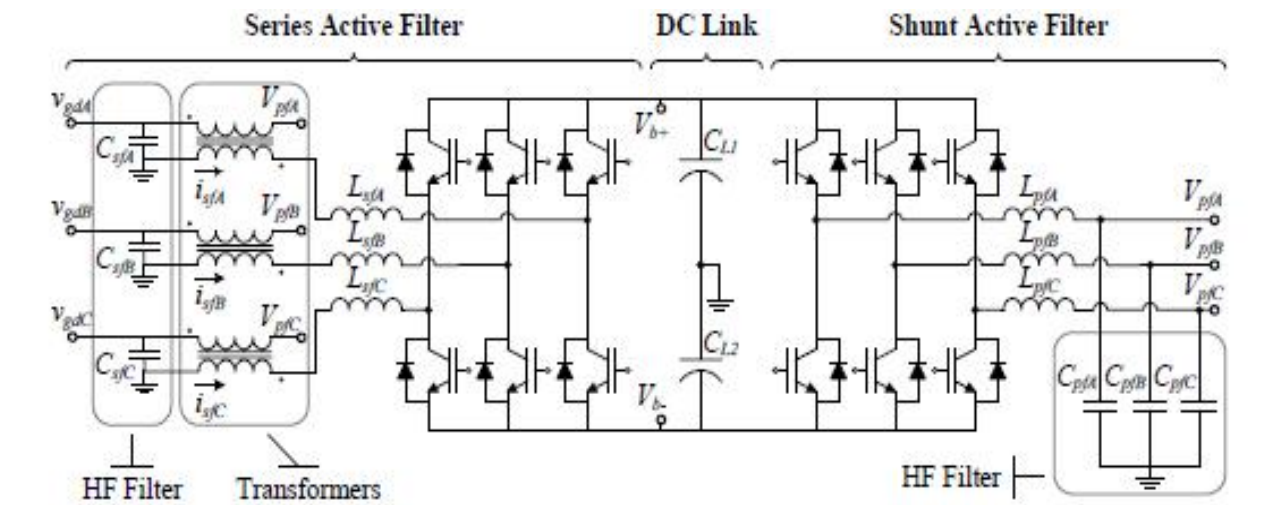

converters connected back-to-back and their respective output filters, as shown in Figure 3.

Three single-phase transformers are used to connect the SAF to the utility grid while the PAF is connected directly to the load. Table 1 shows the specification of the iUPQC.

For this work, a commercial back-to-back power module was used, manufactured by SEMIKRON. The passive compo-nents are shown in Table 2.

Table 1: Design Specifications of the iUPQC

Input line-to-line RMS voltage	V_{in} = 220V
Output nominal power	P_o = 2500VA
DC link voltage	V_b = 400V
Utility grid frequency	f_{grid} = 60Hz
Switching frequency of series and PAFs	f_s = 20kHz
Transformer ratio	n = 1

Table 2: Component Specifications of the Power Modules

Leakage inductance of the SAF coupling transformers	L_{lg} = 2.33mH
Transformer ratio of the SAF coupling Transformers	n = 1
SAF connection inductance	L_{sf} = 650μH
PAF connection inductance	L_{pf} = 650μH
DC Link Capacitance	C_b = 3mF

OUTPUT PASSIVE FILTER DESIGN

The iUPQC circuit can be analyzed by a single phase wiring diagram, as shown in Figure 4. The utility grid impedance is represented by $Z_8 = j\grave{u}L_8 + R_8$, while coupling transformer leakage impedance is represented by *Zlg = jùLlg + Rlg* , and the voltage sources *v8c* and *vp,* represent the equivalent structures of the series and shunt filters, which generates a waveform composed by the fundamental component and by harmonics originated from the commutation of the switches. These high frequencies must be filtered by the output

Figure 4: Single Line Diagram iUPQC

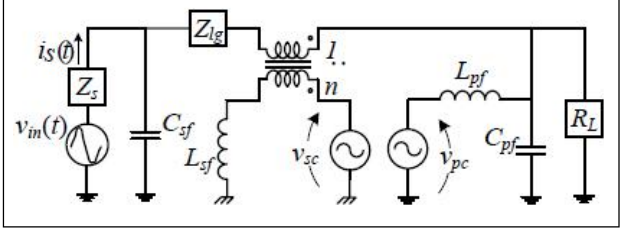

Figure 5: Equivalent Circuit Diagram of SAF

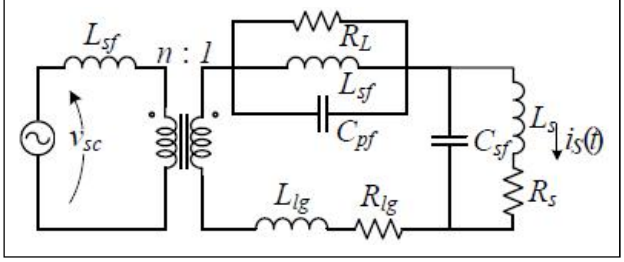

Figure 6: Equivalent Circuit Diagram of PAF

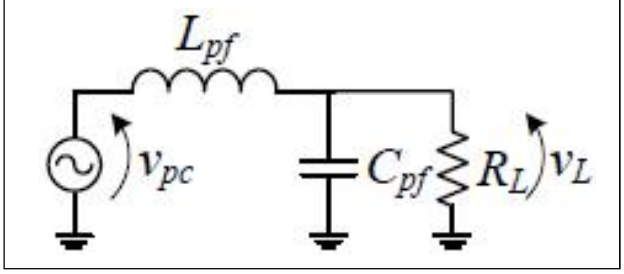

passive filters of the iUPQC ensuring sinusoidal grid currents and load voltages.

Figure 5 shows the equivalent circuit used for the SAF output impedance analysis and Figure 6 shows the equivalent circuit used for the PAF output impedance analysis. In order to simplify the analysis of the PAF the voltage source *v8c* and the inductance L81, which are series connected, were considered as a current source.

Observing the equivalent circuits, we can claim that the PAF output impedance affects the frequency response of the SAF while the

SAF output impedance does not affect the frequency response of the PAF. Therefore the output passive filter design of the iUPQC should be started with the PAF design followed by the SAF design.

The high frequency filter transfer function of the PAF is derived by analyzing the circuit of Figure 6 and shown in Equation (1).

$$\frac{v_L(s)}{v_{pc}(s)} = \frac{1}{L_{pf}C_{pf}} \cdot \frac{1}{s^2 + s \cdot \frac{1}{C_{pf}R_L} + \frac{1}{L_{pf}C_{pf}}} \quad ...(1)$$

The inductor L_{pf} was defined by the power design, so the capacitor C_{pf} will be defined according to the desired cutoff frequency for the filter. In this design, a 2.9 kHz cutoff frequency was used, resulting in a value of 10 µF for the C_{pf} filter capacitor. Figure 7 shows the PAF frequency response for the nominal load and no-load.

The high frequency filter transfer function of the SAF is derived by analyzing the circuit of Figure 5 and shown in Equation (2).

Figure 7: The HP Filter Frequency Response of PAF

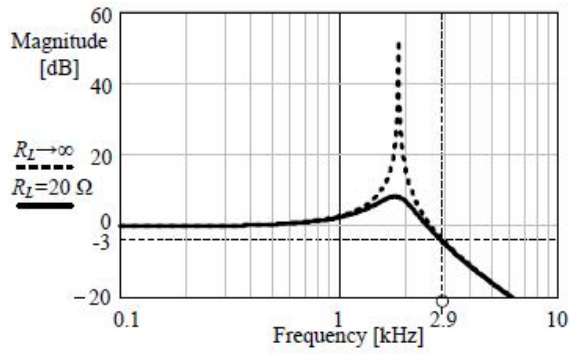

$$\frac{i_s(s)}{v_{sc}(s)} = \frac{n}{\{sL_{sf} + n^2[sL_{lg} + R_{lg} + \alpha + \beta] \cdot \gamma\}} \quad (2)$$

Where:

$$\alpha = \frac{sL_{pf}R_L}{s^2L_{pf}C_{pf}R_L + sL_{sf} + R_L} \quad (3)$$

$$\beta - \frac{sL_{rd} \mid R_{rd}}{s^2L_sC_{sf} + sC_{sf}R_s + 1} \quad (4)$$

$$\gamma = s^2C_{sf}L_s + sC_{sf}R_{lg} + 1 \quad (5)$$

Figure 8: The HP Filter Frequency Response of SAF

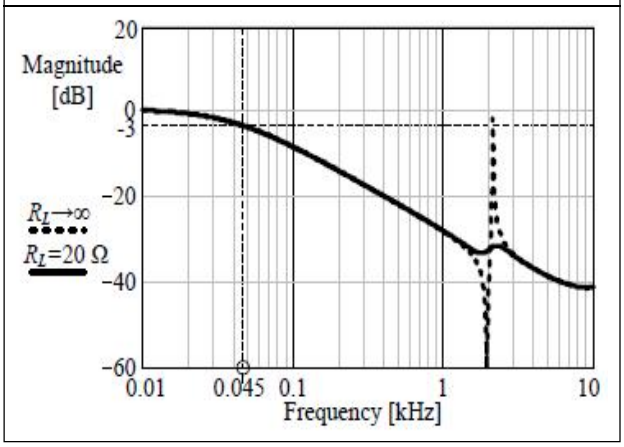

Capacitor C_{pf} will be defined according to the desired cutoff frequency for the filter. In this design a 45 Hz cutoff frequency was used, resulting in a value of 1µF for the C_{pf}. Figure 8 shows the SAF frequency response for nominal load and no-load. It can be noted than the filter response has a low cutoff frequency that can reduce the bandwidth of the SAF, decreasing its effectiveness under operation with harmonics contents on the grid voltage. This characteristic of low frequency attenuation is undesirable and intrinsic to the structure, due to the leakage impedance of the coupling transformers.

An important contribution of this paper and different from what it was stated in some previous articles, which deal with the same iUPQC control strategy, is that in spite of the SAF operates with sinusoidal reference, the control of this filter needs to deal with high

frequency since the current imposed by the SAF is obtained through the voltage imposition on this filter output inductor. The voltage imposed on these inductors is complementary to the utility grid voltage harmonics so that it guarantees a sinusoidal current through the filter. Different from the conventional UPQC whose narrow band frequency control may distort the load voltage, in the iUPQC the narrow band frequency control may distort the current drained from the utility grid. The usage of high power coupling transformers, with low leakage inductance, and the design of higher voltage dc link, allowing the imposition of higher current rate of change on the filter output inductor, are solutions to change the characteristics of the filter attenuation in low frequencies.

PROPOSED CONTROL SCHEME

The proposed iUPQC control structure is an ABC reference frame based control, where SAF and PAF are controlled in an independent way.

In the proposed control scheme, the power calculation and harmonic extraction are not needed since the harmonics, unbal-ances, disturbances and displacement should be compensated.

The SAF has a current loop in order to ensure a sinusoidal grid current synchronized with the grid voltage. The PAF has a voltage loop in order to ensure a balanced, regulated, load voltage with low harmonic distortion. These control loops are independent one from each other since they act independently in each active filter. The dc link voltage control is made in the SAF where the voltage loop determines the amplitude reference for the current loop, in the same mode of the Power Factor Converters (PFC) control schemes. The sinusoidal references for both SAF and PAF controls are generated by a Digital Signal Processor (DSP), which ensure the grid voltage synchronism using a Phase-Locked Loop (PLL).

SAF Control

Figure 9 shows the control block diagrams for the SAF. The SAF control scheme consists of three identical grid current loops and two voltage loops. The current loops are responsible for tracking the reference to each

Figure 9: Control Diagram of SAF

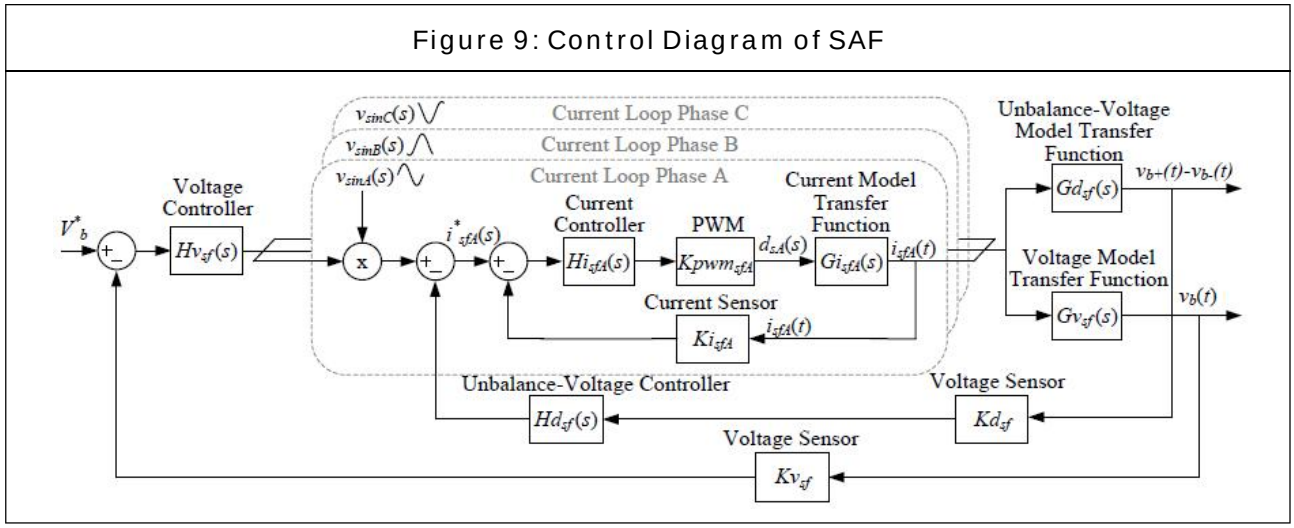

grid input phases, in order to control the grid currents independently. One voltage loop is responsible for regulating the total dc link voltage and the other is responsible for avoiding the unbalances between the dc link capacitors.

The total dc voltage control loop has a low frequency response and determines the reference amplitude for the current loops. Thus, when the load increases overcoming the input grid current, the dc link supply momently the active power consumption resulting in a decreasing of its voltage. This voltage controller acts to increase the grid current reference aiming to restore the dc link voltage. In the same way, when the load decreases, the voltage controller decreases the grid current reference to regulate the dc link voltage. Considering the three-phase input current, sinusoidal and balanced, the voltage loop transfer function is obtained through the method of power balance analysis. The three-phase four wire converter with neutral point can be represented by the circuit shown in Figure 10, composed by a current source which is in parallel with the dc link impedance and whose current source represents the average charge current of dc link.

The resistor R_{pf} is absent in the real circuit (R^{pf-} + oo), it just represents instantaneous active power consumption of dc ink. The term

Figure 10: Equivalent Circuit of SAF Voltage Loop

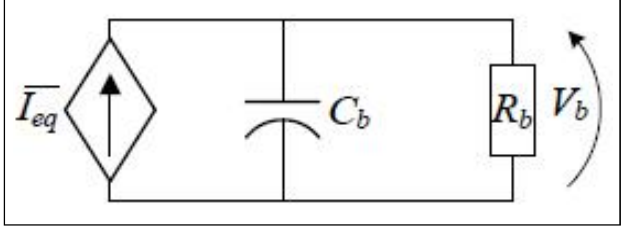

instantaneous is related to time of switching period, since active power consumption of dc link is null for utility grid voltage frequency. The average charge current of dc link is given by Equation (6):

$$\overline{I_{eq}} = \frac{3}{2} \cdot \frac{n \cdot V_{gdpk} \cdot I_{sfpk}}{V_b} \quad ...(6)$$

I_{sfpk} is considered the same for the three phases due to balanced current. Through Equation (6) the voltage loop transfer function is obtained and is represented by Equation (7):

$$Gv_{sf}(s) = \frac{V_b(s)}{I_{sf}(s)} = \frac{3}{2} \cdot n \cdot \frac{V_{gdpk}}{V_b} \cdot \frac{1}{\frac{1}{R_b} + sC_b} \quad ...(7)$$

where

V_{gdbk} - Peak of grid voltage;

$V_b(s)$ - dc link voltage;

R_b - load equivalent resistance;

C_b - Total dc link equivalent capacitance;

n - Transformer ratio;

The open loop transfer function ($OLTF_v$) is given by Equation (8):

$$OLTFv(s) = Gv_{sf}(s) \cdot \frac{Kv_{sf}}{Ki_{sf}} \cdot Km_{sf} \quad ...(8)$$

where

Km_{sf} - Multiplier gain;

Kv_{sf} - Voltage sensor gain;

Ki_{sf} - Current sensor gain;

The Km_{sf} gain is obtained considering the gain of the multiplier integrated circuit and the

peak of the synchronized sinusoidal signal generated by DSP.

Aiming to regulate the total dc link voltage control, a Proportional Integral (PI) + pole controller was designed which ensures a crossover frequency of 4 Hz and phase margin of 45˚. The frequency response of the total voltage loop is shown in Figure 11 including the open loop transfer function ($OLTF_v$), controller transfer function (*Hvsf*) and the compensated loop transfer function ($OLTF_v$ + *Hvsf*).

The unbalanced-voltage control loop also has a low frequency loop and acts on the dc level of the grid current reference in order to keep the voltage equilibrium in dc link capacitors. When a voltage unbalance occurs, this loop adds a dc level to the references of the grid currents aiming to equalize both *CL1* and *CL2* voltages.

The unbalanced-voltage loop transfer function is obtained through the analysis of the simplified circuit shown in Figure 12. The four wire converter allows the single-phase analysis, where two current sources represent the current on the inverter switches. In Figure 12 the current $i_{sc}(t)$ represents the current through the neutral point and *d(t)* represents the duty cycle.

Figure 11: Voltage Loop Frequency Response of the SAF

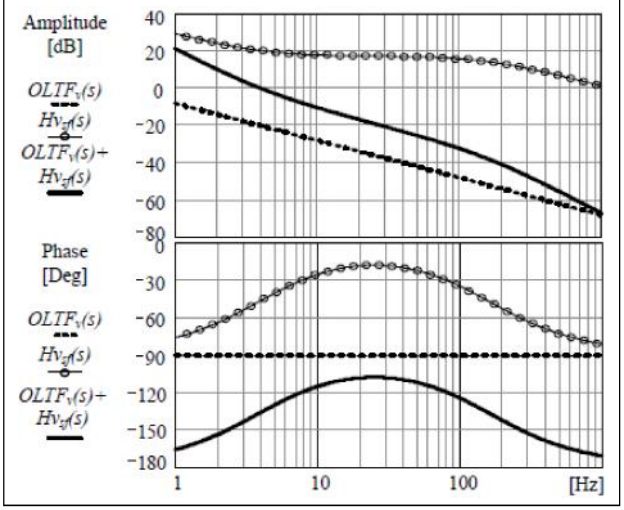

Through the mesh analysis and applying Laplace, the unbalanced-voltage loop transfer function is obtained and given by Equation (9):

$$Gd_{sf}(s) = \frac{V_{b1}(s) - V_{b2}(s)}{I_{sc}(s)} = \frac{3}{2 \cdot s \cdot C_b} \quad ...(9)$$

The open loop transfer function (*OLTFd*) is given by

$$OLTF_d(s) = Gd_{sf}(s) \cdot \frac{Kd_{sf}}{Ki_{sf}} \quad ...(10)$$

where:

Kd_{sf} - Differential voltage sensor gain;

Aiming to eliminate the differential dc link voltage, a PI + pole controller was designed which ensures a crossover frequency of 0.5 Hz and phase margin of 50˚.

The current control scheme consists of three identical cur-rent loops, except for the 120 degree phase displacements from

Figure 12: Equivalent Circuit of SAF Unbalanced-Voltage Loop

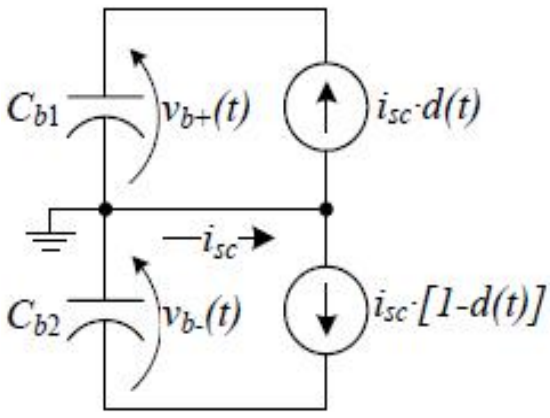

Figure 13: Unbalance-Voltage Loop Frequency Response of the SAF

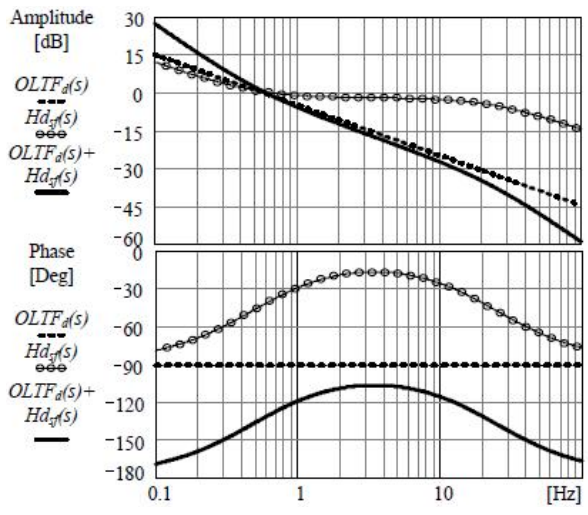

Figure 14: Single Phase Equivalent Circuit Diagram of SAF

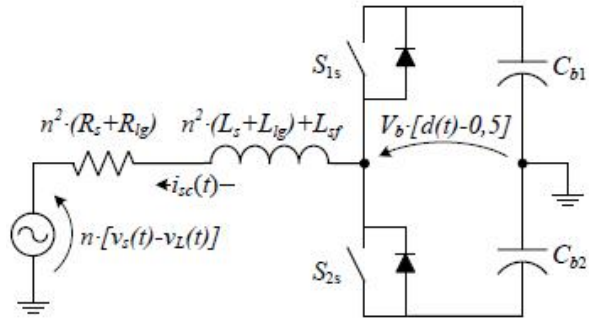

references of each other. The current loops have a fast response to track the sinusoidal references, allowing the decoupling analysis in relation to the voltage loop. The current loop transfer function is obtained through the analysis of the single-phase equivalent circuit shown in Figure 14.

The voltage source represents the voltage on the coupling transformer. The dynamic model is obtained through the circuit analysis using average values related to switching period. Under these conditions, the voltages $v_s(t)$ and $vL(t)$ are constants. Through small signal analysis and using Laplace, the current loop transfer function is given by Equation (11):

$$Gi_{fs}(s) = \frac{I_{sc}(s)}{D(s)} = \frac{V_b}{sA_1 + n^2 \cdot (R_s + R_{lg})} \quad (11)$$

Where:

$$A_1 = n^2 \cdot (L_s + L_{lg}) + L_{sf} \quad (12)$$

response of the differential voltage loop is shown in Figure 13, including the open loop transfer function (*OLTFd*), controller transfer function (*Hdsf*) and the compensated loop transfer function (*OLTFd* + *Hdsf*).

and:

L_s - Series grid inductance;

R_s - Series grid resistance;

L_{lg} - Leakage inductance of the coupling transformer;

R_{lg} - Series resistance of the coupling transformer;

The open loop transfer function (*OLTFi*) is given by Equation (13):

$$OLTFi(s) = Gisf(s)\ Kpwm_sf\ Kisf \quad ...(13)$$

where

$Kpwm_sf$ - Series filter PWM modulator gain;

The $Kpwm_sf$ gain equals the inverse peak value of the triangular carrier.

Aiming to track the current reference, a PI + pole controller was designed which ensures a crossover frequency of 5 kHz and phase margin of 70°. The frequency response of the current loop is shown in Figure 15 including the open loop transfer function ($OLTF_{vpf}$), controller transfer function (H_{vpf}) and the compensated loop transfer function ($OLTF_{vpf}$+ H_{vpf}).

Figure 15: Current Loop Frequency Response of SAF

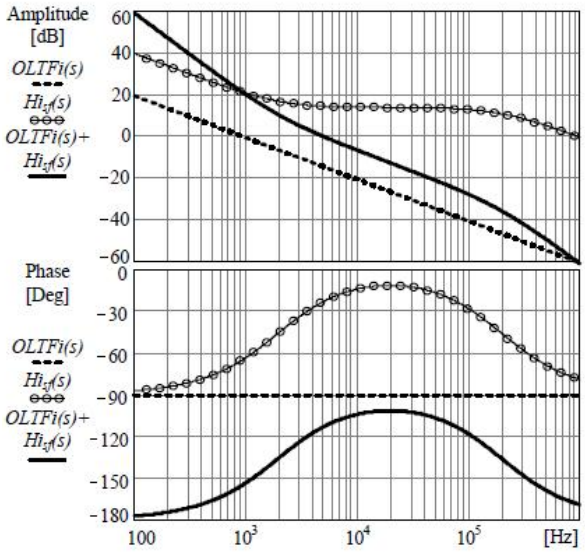

PAF Control

The PAF control scheme is formed by three identical load voltage feedback loops, except for the 120 degree phase displacements from references of each other. The voltage loops are responsible for tracking the sinusoidal voltage reference for each load output phases, in order to control the load voltages independently.

The voltage loop transfer function is obtained through the analysis of the single-phase equivalent circuit show in Figure 17. The dynamic model is obtained through the circuit analysis using average values related to switching period. Through small signal analysis and using Laplace, the voltage loop transfer function is given by Equation (14):

$$Gv_{pf}(s) = \frac{V_b}{L_{pf}C_{pf}} \cdot \frac{1}{s^2 + s\left(\frac{1}{C_{pf}R_L}\right) + \frac{1}{L_{pf}C_{pf}}} \quad ...(14)$$

where $Gv_{pf}(s) = V_b(s)/D(s)$

The open loop transfer function ($OLTFv_sf$) is given by Equation (15):

Figure 16: Shows the Control Block Diagram of the Shunt Active Filter Controller

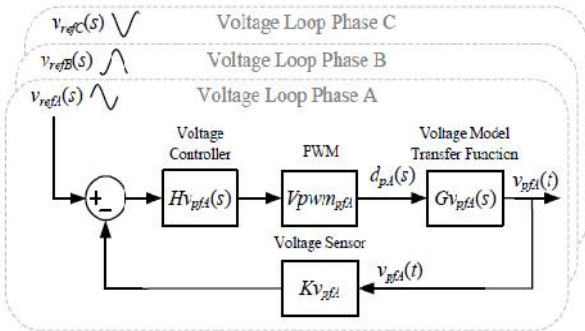

Figure 17: Single Phase Equivalent Circuit of PAF

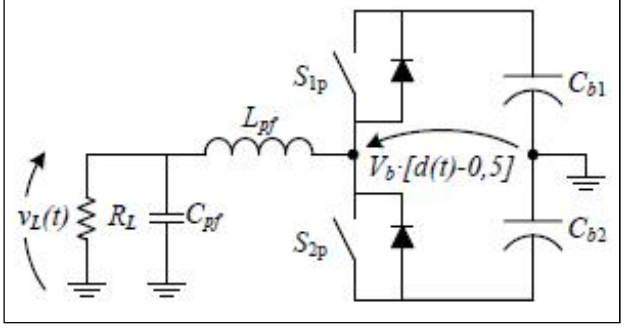

Figure 18: Voltage Loop Frequency Response of SAF

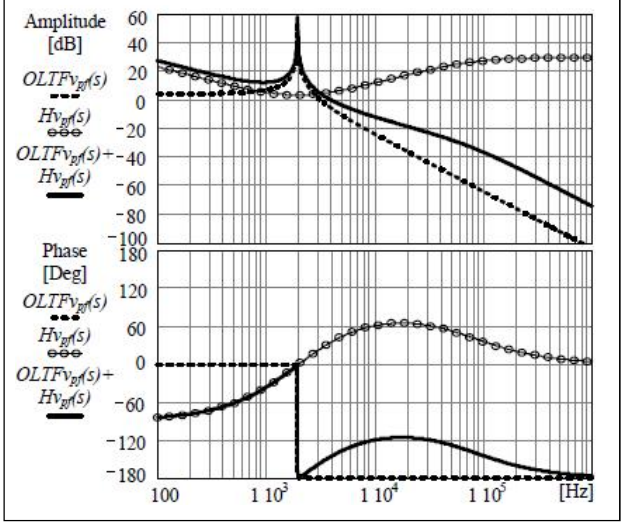

$$OLTFv(s) = Gv_{pf}(s) \cdot Kpwm_sf \cdot Kv_{sf} \quad ...(15)$$

where

$Kpwm_sf$ - Shunt filter PWM modulator gain;

Aiming to track the voltage reference, a Proportional Integral Derivative (PID) + additional pole controller was designed which ensures a crossover frequency of 4 kHz and phase margin of 35˚.

The voltage loop frequency response is shown in Figure 18 including the open loop transfer function ($OLTFv_sf$), controller transfer function (Hv_sf) and the compensated loop transfer function ($OLTFv_sf + Hv_sf$).

SIMULATION RESULTS

Figure 20: Circuit Diagram

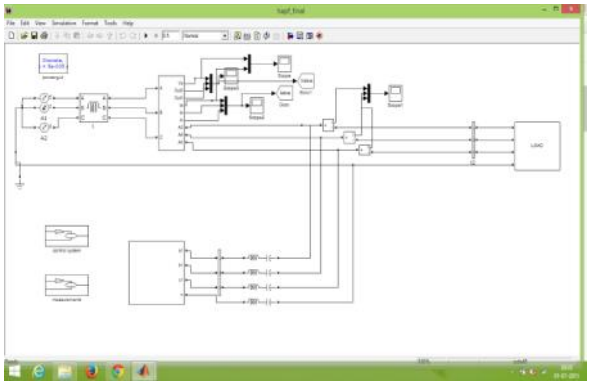

Figure 21: Input Voltage and Current

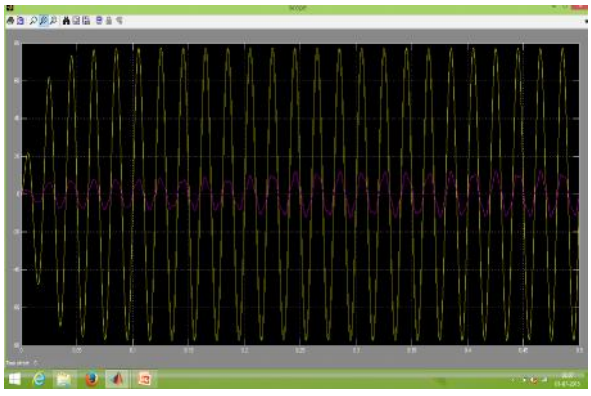

Figure 22: Load Currents

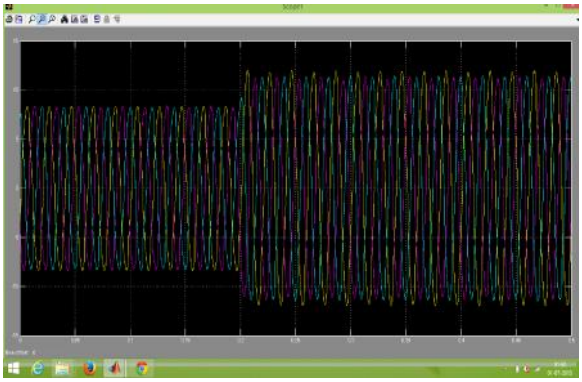

THE PROPOSED HYBRID PID PLUS FUZZY CONTROL

In the fuzzification process, we only employ three input membership functions μ_{N_x}, μ_{Z_x} and μ_{P_x} shown in Figure 3 to map a crisp input to a fuzzy set with a degree of certainty where x = g(t) or $\Delta g(t)$ with g(t) = K1f(t) and $\Delta g(t) = K2\Delta f$ (t). Those three membership functions are chosen because of their simplicity for computation since a large number of membership functions and rules can cause high computational burden for a fuzzy controller. For any x ∈ N where N denotes the interval (– ∞,0] , its corresponding linguistic value is 'N'. Moreover, for any x ∈ P where P denotes the interval (0, ∞) , its corresponding linguistic value is 'P'. For any x ∈ Z where Z denotes the interval [–b, b], its corresponding linguistic value is 'Z'. The membership functions, μ_{Z_x} and μ_{P_x} are given by

$$\mu_N(x) = \begin{cases} 1 & x \le -b \\ \frac{-x}{b} & -b < x \le 0 \\ 0 & \text{otherwise.} \end{cases}$$

$$\mu_Z(x) = \begin{cases} \frac{x+b}{b} & -b < x \le 0 \\ \frac{b-x}{b} & 0 < x \le b \\ 0 & \text{otherwise.} \end{cases}$$

$$\mu_P(x) = \begin{cases} 1 & b \le x \\ \frac{x}{b} & 0 < x \le b \\ 0 & \text{otherwise.} \end{cases}$$

The fuzzy inference engine, based on the input fuzzy sets in combination with the expert's experience, uses adequate IF-THEN rules in the knowledge base to make decisions and produces an implied output fuzzy set *u*. For this particular application, the proposed IF-THEN fuzzy rule base is shown in Table 3 and is described as follows:

i. If $\Delta g(t) \in$ N, then $u(g(t), \Delta g(t)) = b$.
ii. If $\Delta g(t) \in$ P, then $u(g(t), \Delta g(t)) = -b$.
iii. If $\Delta g(t) \in$ Z and $g(t) \in$ N, then $u(g(t), \Delta g(t)) = -b$ ..
iv. If $\Delta g(t) \in$ Z and $g(t) \in$ P, then $u(g(t), \Delta g(t)) = b$.
v. If $\Delta g(t) \in$ Z and $g(t) \in$ Z, then $u(g(t), \Delta g(t)) = 0$.

Moreover, the Mamdani-type min operation for fuzzy inference is employed in this study.

Figure 23: The Block Diagram of the Proposed Controller

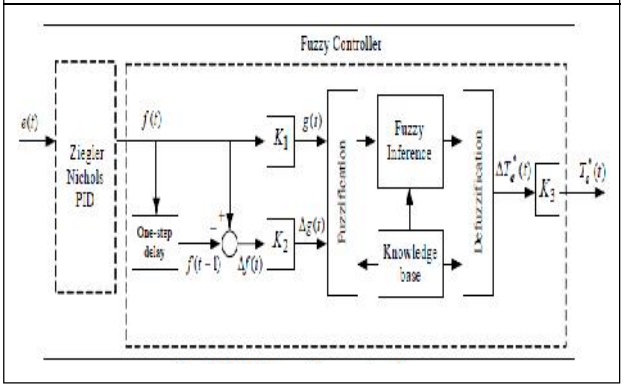

Figure 24: Membership Functions with x = g(t) or ag(t)

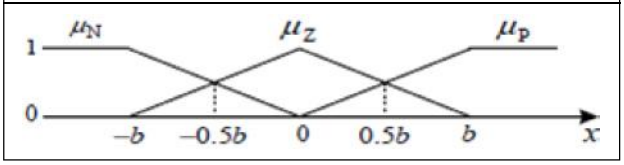

In the de fuzzification process, we employ the' center of mass' de fuzzification method for transforming the implied output fuzzy set into a crisp output, and obtain

Table 3: Fuzzy Rule Base

g(t) / Δg(t) / u	N	Z	P
N	b	b	b
Z	-b	0	b
P	-b	-b	-b

$$\Delta T_e^*(t) = \frac{\sum_{i \in FL(g(t))} \sum_{j \in FL(\Delta g(t))} \min\{\mu_i(g(t)), \mu_j(\Delta g(t))\} \times u(i,j)}{\sum_{i \in FL(g(t))} \sum_{j \in FL(\Delta g(t))} \min\{\mu_i(g(t)), \mu_j(\Delta g(t))\}}$$

$$FL(a) = \begin{cases} \{N, Z\} & \text{if } a \in N \text{ and } a \in Z \\ \{P, Z\} & \text{if } a \in P \text{ and } a \in Z \\ \{N\} & \text{if } a \in N \text{ and } a \notin Z \\ \{P\} & \text{if } a \in P \text{ and } a \notin Z. \end{cases}$$

The output of the fuzzy controller is given by

$$T_e^*(t) = K_3 \cdot \Delta T_e^*(t)$$

CONCLUSION

The design of a Unified Power Quality Conditioner (UPQC) connected system has been presented in this project. Where iupqc is installed to compensate the different power quality problems, which may play an important role in future upqc based distribution system. The simulation results shows that the distorted and unbalanced load currents seen from the utility side act as perfectly balanced source currents and are free from distortion. Here we can absorb the power quality problems like voltage and current unbalanced and reduced the Total Harmonic Distortion (THD) of system connected tot the UPQC. The work can be extended to compensate the supply voltage and load current imperfections such as sags,

swells, interruptions, voltage imbalance, flicker, and current unbalance.

Comparison between with and without fuzzy controller:

	Without Fuzzy	**With Fuzzy**
Input voltage	180 v	180 v
Input current	24A	24A
THD	7.9%	6.0%

REFERENCES

1. Fujita H and Akagi H (1998), "The Unified Power Quality Conditioner: The Integration of Series and Shunt-Active Filters", *IEEE Trans. on Power Electron.*, Vol. 13, No. 2, pp. 315-322.
2. Han B, Bae B, Baek S and Jang G (2006), "New Configuration of UPQC for Medium-Voltage Application", *IEEE Trans. on Power Deliv.*, Vol. 21, No. 3, pp. 1438-1444.
3. Chakraborty S, Weiss M and Simoes M (2007), "Distributed Intelligent Energy Management System for a Single-Phase High-Frequency ac Microgrid", *IEEE Trans. on Ind. Electron.*, Vol. 54, No. 1, pp. 97-109.
4. Forghani M and Afsharnia S (2007), "Online Wavelet Transform-Based Control Strategy for UPQC Control System", *IEEE Trans. on Power Deliv.*, Vol. 22, No. 1, pp. 481-491.
5. Jindal A, Ghosh A and Joshi A (2007), "Interline Unified Power Quality Conditioner", *IEEE Trans. on Power Deliv.*, Vol. 22, No. 1, pp. 364-372.
6. Kolhatkar Y and Das S (2007), "Experimental Investigation of a Single-Phase UPQC with Minimum va Loading", *IEEE Trans. on Power Deliv.*, Vol. 22, No. 1, pp. 373-380.
7. Basu M, Das S and Dubey G (2008), "Investigation on the Performance of UPQC-q for Voltage Sag Mitigation and Power Quality Improvement at a Critical Load Point", *IET Generation Transmission Distribution*, Vol. 2, No. 3, pp. 414-423.
8. Khadkikar V and Chandra A (2008), "A New Control Philosophy for a Unified Power Quality Conditioner (UPQC) to Coordinate Load-Reactive Power Demand Between Shunt and Series Inverters", *IEEE Trans. on Power Deliv.*, Vol. 23, No. 4, pp. 2522-2534.
9. Aredes M and Fernandes R (2009), "A Dual Topology of Unified Power Quality Conditioner: The iUPQC", in *13th European Conf. on Power Electron. and Appl.*, September, pp. 1-10.
10. Brenna M, Faranda R and Tironi E (2009), "A New Proposal for Power Quality and Custom Power Improvement: Open UPQC", *IEEE Trans. on Power Deliv.*, Vol. 24, No. 4, pp. 2107-2116.
11. Chakraborty S and Simoes M (2009), "Experimental Evaluation of Active Filtering in a Single-Phase High-Frequency ac Microgrid", *IEEE Trans. on Energy Conversion*, Vol. 24, No. 3, pp. 673-682.
12. Khadkikar V and Chandra A (2009), "A Novel Structure for Three-Phase Four-Wire Distribution System Utilizing Unified Power Quality Conditioner (UPQC)", *IEEE*

Trans. on Ind. Appl., Vol. 45, No. 5, pp. 1897-1902.

13. Kwan K H, Chu Y C and So P L (2009), "Model-Based H Control of a Unified Power Quality Conditioner", *IEEE Trans. on Ind. Electron.*, Vol. 56, No. 7, pp. 2493-2504.

14. Munoz J, Espinoza J, Moran L and Baier C (2009), "Design of a Modular UPQC Configuration Integrating a Components Economical Analysis", *IEEE Trans. on Power Deliv.*, Vol. 24, No. 4, pp. 1763-1772.

15. Axente I, Ganesh J, Basu M, Conlon M and Gaughan K (2010), "A 12-kva dsp-Controlled Laboratory Prototype UPQC Capable of Mitigating Unbalance in Source Voltage and Load Current", *IEEE Trans. on Power Electron.*, Vol. 25, No. 6, pp. 1471-1479.

16. Axente I, Basu M, Conlon M and Gaughan K (2010), "Protection of Unified Power Quality Conditioner Against the Load Side Short Circuits", *IET Power Electron.*, Vol. 3, No. 4, pp. 542-551.

17. Karanki S, Mishra M and Kumar B (2010), "Particle Swarm Optimization-Based Feedback Controller for Unified Power-Quality Conditioner", *IEEE Trans. on Power Deliv.*, Vol. 25, No. 4, pp. 2814-2824.

18. Lee W C, Lee D M and Lee T-K (2010), "New Control Scheme for a Unified Power-Quality Compensator-q with Minimum Active Power Injection", *IEEE Trans. on Power Deliv.*, Vol. 25, No. 2, pp. 1068-1076.

19. Franca B and Aredes M (2011), "Comparisons Between the UPQC and its Dual Topology (iUPQC) in Dynamic Response and Steady-State", in *IECON 37th Annu. Conf. on IEEE Ind. Electron.*, November, pp. 1232-1237.

20. Kesler M and Ozdemir E (2011), "Synchronous-Reference-Frame-Based Control Method for UPQC Under Unbalanced and Distorted Load Conditions", *IEEE Trans. on Ind. Electron.*, Vol. 58, No. 9, pp. 3967-3975.

21. Khadkikar V and Chandra A (2011), "UPQC-s: A Novel Concept of Simultaneous Voltage Sag/Swell and Load Reactive Power Compensations Utilizing Series Inverter of UPQC", *IEEE Trans. on Power Electron.*, Vol. 26, No. 9, pp. 2414-2425.

22. Khadkikar V, Chandra A, Barry A and Nguyen T (2011), "Power Quality Enhancement Utilising Single-Phase Unified Power Quality Conditioner: Digital Signal Processor-Based Experimental Validation", *IET Power Electron.*, Vol. 4, No. 3, pp. 323-331.

23. Kinhal V, Agarwal P and Gupta H (2011), "Performance Investigation of Neural-Network-Based Unified Power-Quality Conditioner", *IEEE Trans. on Power Deliv.*, Vol. 26, No. 1, pp. 431-437.

24. Leon A, Amodeo S, Solsona J and Valla M (2011), "Non-Linear Optimal Controller for Unified Power Quality Conditioners", *IET Power Electron.*, Vol. 4, No. 4, pp. 435-446.

25. Khadkikar V (2012), "Enhancing Electric Power Quality Using UPQC: A

Comprehensive Overview", *IEEE Trans. on Power Electron.*, Vol. 27, No. 5, pp. 2284-2297.

26. Kwan K H, So P L and Chu Y C (2012), "An Output Regulation-Based Unified Power Quality Conditioner with Kalman Filters", *IEEE Trans. on Ind. Electron.*, Vol. 59, No. 11, pp. 4248-4262.
27. Li G, Ma F, Choi S and Zhang X (2012), "Control Strategy of Across-Phase-Connected Unified Power Quality Conditioner", *IET Power Electron.*, Vol. 5, No. 5, pp. 600-608.
28. Munoz J, Espinoza J, Baier C, Moran L, Espinosa E, Melin P and Sbarbaro D (2012), "Design of a Discrete-Time Linear Control Strategy for a Multicell UPQC", *IEEE Trans. on Ind. Electron.*, Vol. 59, No. 10, pp. 3797-3807.
29. Karanki K, Geddada G, Mishra M and Kumar B (2013), "A Modified Three-Phase Four-Wire UPQC Topology with Reduced dc-link Voltage Rating", *IEEE Trans. on Ind. Electron.*, Vol. 60, No. 9, pp. 3555-3566.
30. Dias J, Busarello T D C, Michels L, Rech C and Mezaroba M (2011), "Unified Power Quality Conditioner Using Simplified Digital Control", *SOBRAEP Trans.*, Vol. 16, p. 9.
31. Dai K, Liu P, Wang G, Duan S and Chen J (2004), "Practical Approaches and Novel Control Schemes for a Three-Phase Three-Wire Series-Parallel Compensated Universal Power Quality Conditioner", in *APEC'04 Appl. Power Electron. Conf. and Expo.*, Vol. 1, pp. 601-606.
32. Pottker de Souza F and Barbi I (2000), "Single-Phase Active Power Filters for Distributed Power Factor Correction", in *PESC Power Electron. Spec. Conf.*, Vol. 1, pp. 500-505.
33. Moran S (1989), "A Line Voltage Regulator/Conditioner for Harmonic-Sensitive Load Isolation", in *Conf. Rec. IEEE Ind. Appl. Annu. Meeting.*, Vol.1, October, pp. 947-951.
34. Kamran F and Habetler T (1998), "A Novel on-Line Ups with Universal Filtering Capabilities", *IEEE Trans. on Power Electron.*, Vol. 13, No. 3, pp. 410-418.
35. da Silva S, Donoso-Garcia P, Cortizo P and Seixas P (2002), "A Three-Phase Line-Interactive Ups System Implementation with Series-Parallel Active Power-Line Conditioning Capabilities", *IEEE Trans. on Ind. Appl.*, Vol. 38, No. 6, pp. 1581-1590.